

Supporting Information

Figure S1 The experimental PXRD and the simulated patterns of the three anhydrous forms of non-stoichiometric PDA-OPA salt (left). The two photos on the right show the crystal habit of the corresponding crystal forms, respectively.

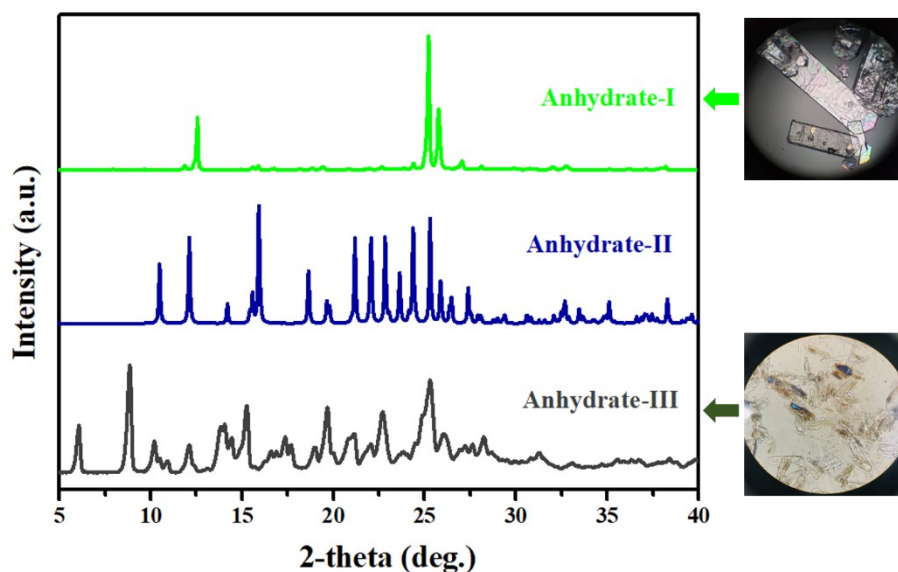


Figure S2 Characteristic FTIR patterns of the two PDA-OPA anhydrous forms.

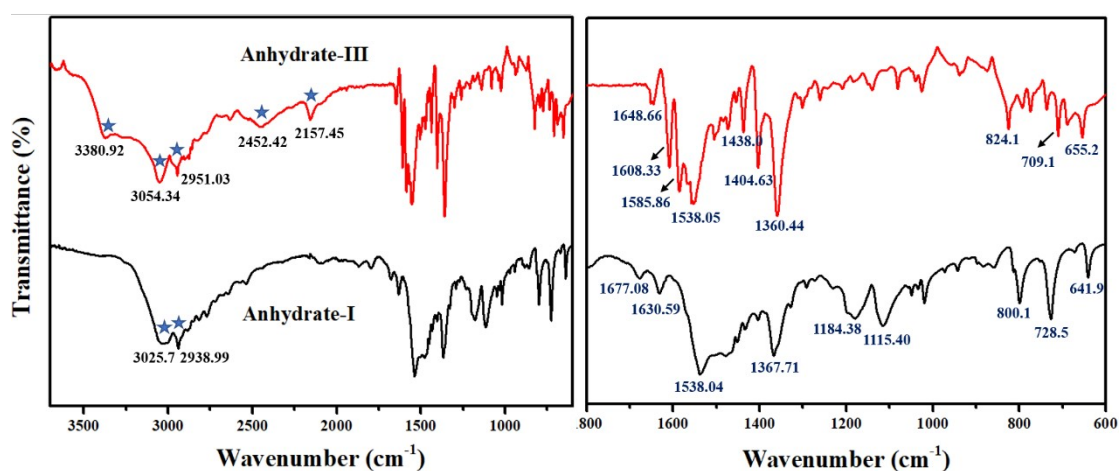


Table S1 Crystallographic data for PDA-OPA two anhydrous crystal forms.

	Anhydrate-I	Anhydrate-II
Empirical formula	C ₂₁ H ₂₄ O ₈ N ₂	C ₂₁ H ₂₄ O ₈ N ₂
Formula weight	434.44	434.44
Crystal system	monoclinic	monoclinic
Space group	C2/c	Cc
<i>a</i> (Å)	15.2457(12)	11.3309(9)
<i>b</i> (Å)	18.4249(14)	12.4114(11)
<i>c</i> (Å)	8.4299(6)	14.7248(12)
α (deg)	90	90
β (deg)	110.730(5)	90.451(2)
γ (deg)	90	90
Volume (Å ³)	2214.7(3)	2070.7(3)
<i>Z</i>	4	4
<i>D</i> _{calc.} (g/cm ³)	1.303	1.394
μ (mm ⁻¹)	0.101	0.108
F (000)	920	920
Observed data [1179	2627
<i>R</i> (int)	0.050	0.034
<i>R</i> _I [<i>I</i> > 2 σ (<i>I</i>)]	0.0592	0.0381
<i>wR</i> ²	0.1397	0.0999
GOF on F ²	1.03	1.08
Diff density	-0.17, 0.19	-0.18, 0.17
CCDC	2106410	2006386

Table S2 Hydrogen-bond geometry for six different crystal forms of PDA-OPA.

D—H \cdots A	D(D-H) / Å	d(H \cdots A) / Å	d(D \cdots A) / Å	D—H \cdots A
MeOH solvate				
N1—H1A \cdots O6	0.8900	2.0100	2.855(3)	159.00
N1—H1B \cdots O2	0.8900	1.9100	2.789(3)	168.00
N1—H1C \cdots O3	0.8900	1.9800	2.844(3)	163.00
N2—H2A \cdots O5	0.8900	2.2000	2.990(3)	148.00
N2—H2A \cdots O6	0.8900	2.1800	2.963(3)	146.00
N2—H2B \cdots O3	0.8900	2.2800	3.058(3)	146.00
N2—H2C \cdots O3	0.8900	1.9700	2.853(3)	176.00

N3—H3A…O4	0.8900	1.9300	2.801(4)	164.00
N3—H3B…O1	0.8900	1.9000	2.767(3)	166.00
N3—H3C…O7	0.8900	1.8700	2.703(3)	156.00
N4—H4A…O5	0.8900	1.9300	2.801(3)	168.00
N4—H4B…O2	0.8900	1.9300	2.797(3)	162.00
N4—H4C…O7	0.8900	2.4900	3.051(4)	121.00
N4—H4C…O8	0.8900	2.0400	2.925(4)	178.00
O9—H9…O8	0.8200	1.9400	2.720(4)	159.00
C8—H8…O1	0.9300	2.4900	2.801(3)	100.00

Anhydrate-I

N1—H1A…O3	0.8900	2.4600	3.122(3)	131.00
N1—H1A…O4	0.8900	2.0100	2.894(3)	170.00
N1—H1B…O1	0.8900	1.9100	2.783(3)	165.00
N1—H1C…O2	0.8900	1.9300	2.822(3)	179.00
O3—H3…O2	0.8200	1.5900	2.407(3)	172.00
C5—H5…O4	0.9300	2.3400	2.714(4)	104.00
C8—H8…O1	0.9300	2.3700	2.737(4)	103.00

Anhydrate-II

N1—H1A…O3	0.8900	2.0200	2.812(3)	148.00
N1—H1B…O1	0.8900	1.8200	2.701(3)	172.00
N1—H1C…O6	0.8900	2.1500	2.838(3)	133.00
N1—H1C…O7	0.8900	2.3100	2.846(3)	119.00
N2—H2A…O5	0.8900	1.8400	2.719(3)	168.00
N2—H2B…O8	0.8900	1.8800	2.757(3)	170.00
N2—H2C…O2	0.8900	2.2600	2.873(3)	126.00
N2—H2C…O4	0.8900	2.5200	3.051(3)	119.00
O4—H4…O6	0.8200	1.6700	2.484(3)	171.00
O7—H7…O2	0.8200	1.6700	2.480(3)	168.00
C7—H7A…O3	0.9300	2.5400	3.287(4)	137.00

Monohydrate

N1—H1A…O5	0.8900	1.8500	2.721(5)	165.00
N1—H1B…O1	0.8900	1.8200	2.672(4)	160.00

N1—H1C…O2	0.8900	1.8900	2.765(4)	167.00
N2—H2A…O1	0.8900	2.0200	2.882(4)	164.00
N2—H2B…O3	0.8900	1.8300	2.677(4)	158.00
N2—H2C…O4	0.8900	2.0500	2.834(4)	146.00
O5—H5C…O2	0.8500	1.9100	2.748(4)	169.00
O5—H5D…O4	0.8500	1.8700	2.711(5)	169.00

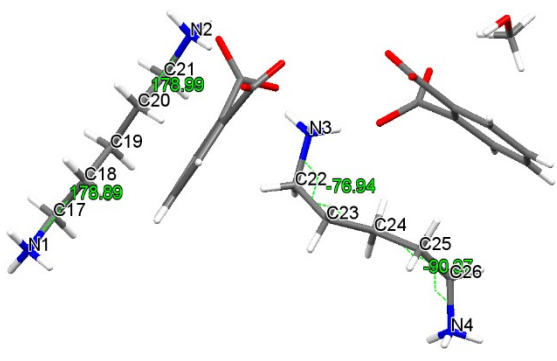
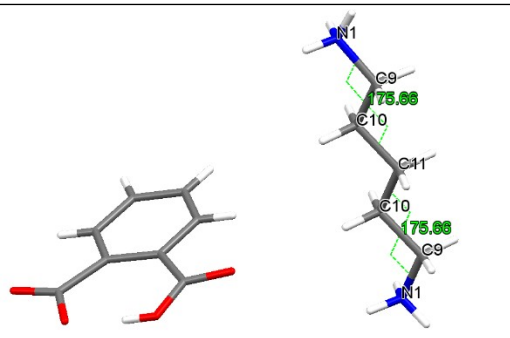
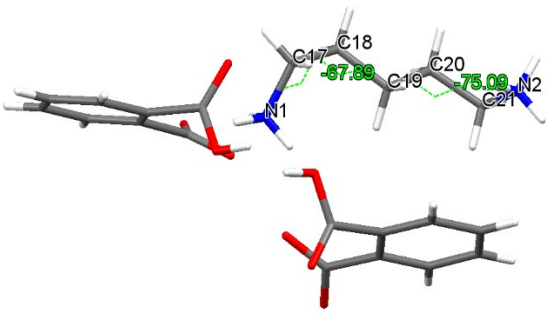
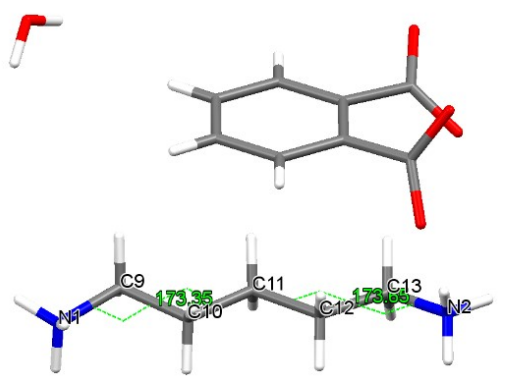
Dihydrate

N1—H1A…O3	0.8900	2.0400	2.888(3)	159.00
N1—H1B…O1	0.8900	1.8300	2.719(3)	175.00
N1—H1C…O4	0.8900	1.9800	2.841(3)	164.00
N2—H2A…O6	0.8900	1.9500	2.792(3)	158.00
N2—H2B…O2	0.8900	2.0000	2.868(3)	164.00
N2—H2C…O5	0.8900	1.9700	2.831(3)	162.00
O5—H5C…O3	0.8500	1.8300	2.669(3)	172.00
O5—H5D…O4	0.8500	1.8300	2.673(3)	172.00
O6—H6C…O1	0.8500	1.9400	2.790(3)	177.00
O6—H6D…O5	0.8500	1.8900	2.742(3)	177.00
C8—H8…O1	0.9300	2.4600	2.772(4)	100.00

Trihydrate

N1—H1A…O7	0.8900	1.9500	2.815(3)	165.00
N1—H1B…O2	0.8900	1.9800	2.853(3)	168.00
N1—H1C…O3	0.8900	1.9200	2.803(3)	171.00
N2—H2A…O1	0.8900	1.9300	2.807(3)	170.00
N2—H2B…O6	0.8900	2.2900	3.005(3)	138.00
N2—H2B…O5	0.8900	2.2800	2.917(3)	129.00
N2—H2C…O4	0.8900	2.0800	2.855(3)	145.00
O5—H5C…O4	0.8500	1.9300	2.780(2)	179.00
O5—H5D…O3	0.8500	1.9300	2.784(2)	179.00
O6—H6C…O2	0.8500	1.9300	2.766(3)	170.00
O6—H6D…O1	0.8500	1.9000	2.737(3)	170.00
O7—H7C…O5	0.8500	1.9600	2.809(3)	176.00
O7—H7D…O6	0.8500	1.9500	2.797(3)	175.00

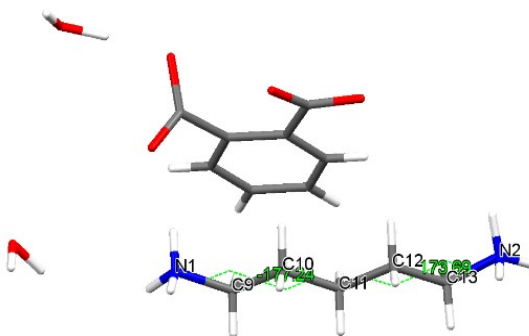
Table S3 Comparison of the torsion angles of PDA species in various solid forms.

	Torsion angle (°)	Structure
MeOH solvate	N1-C17-C18-C19: 178.89	
	N2-C21-C20-C19: 178.99	
	N3-C22-C23-C24: -76.94	
	N4-C26-C25-C24: -90.97	
Anhydrate-I	N1-C9-C10-C11: 175.66	
Anhydrate-II	N1-C17-C18-C19: -67.89	
	N2-C21-C20-C19: -75.09	
Monohydrate	N1-C9-C10-C11: 173.35	
	N2-C13-C12-C11: 173.65	

Dihydrate

N1-C9-C10-C11: -177.24

N2-C13-C12-C11: 173.69



Trihydrate

N1-C9-C10-C11: 178.99

N2-C13-C12-C11: 168.07

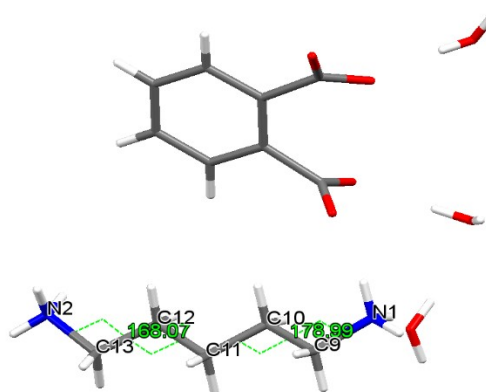


Figure S3 Analysis of Intermolecular interaction interactions, hydrogen bonding and synthons, and crystal packing patterns of anhydrate-I of PDA-OPA (1:2). (a) Asymmetric unit, (b) 1D structure, (c) 2D structure with synthons motifs and (d) 3D supramolecular framework marked by the yellow colour, viewing along the (001) crystallographic direction. (e-f) $\pi\cdots\pi$ interactions are shown as orange dashed line view along the (001) face and the packing view along the (011) crystallographic direction.

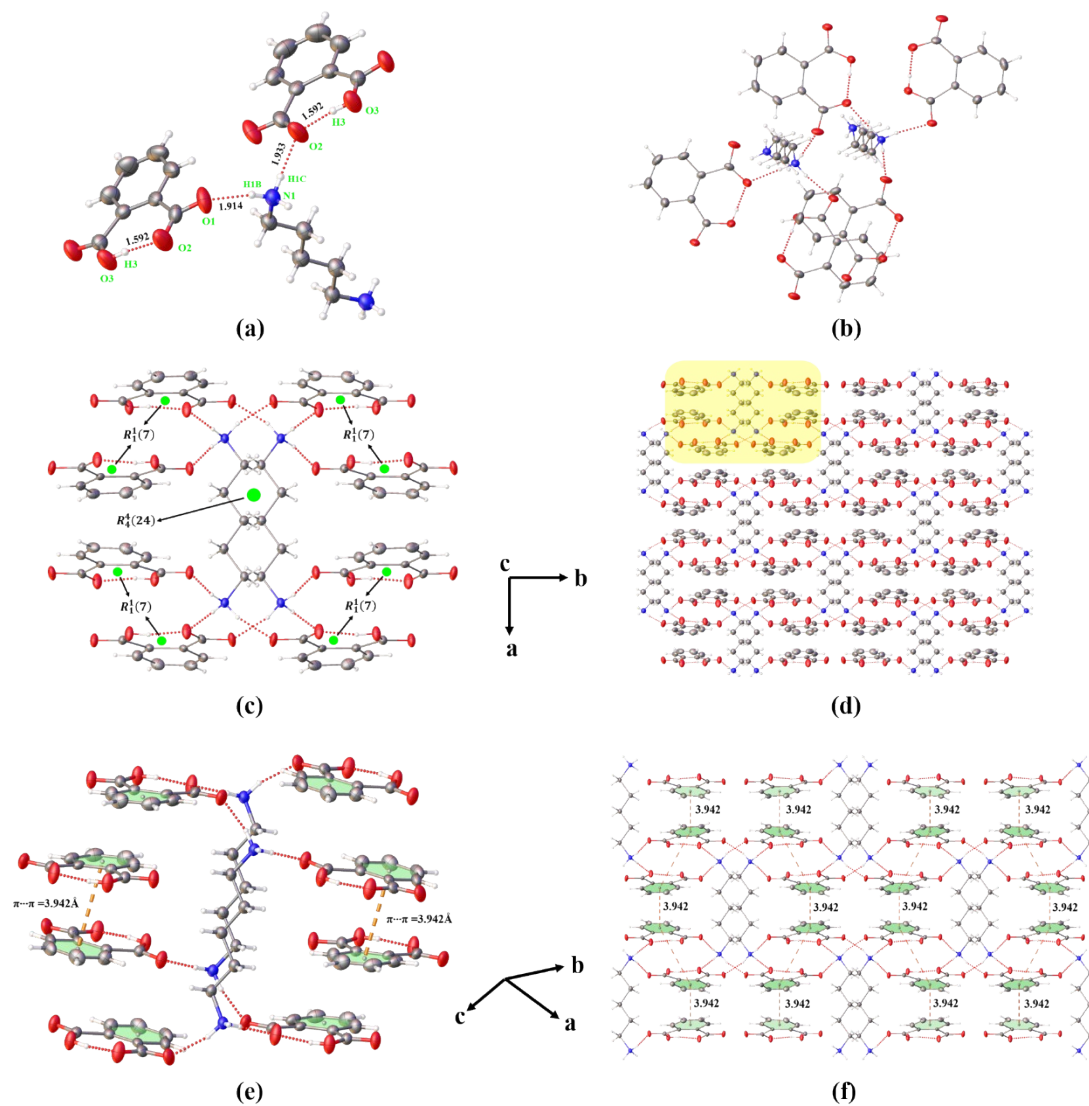


Figure S4 Analysis of Intermolecular interaction interactions, hydrogen bonding and synthons, and crystal packing patterns of anhydrate-II of PDA-OPA (1:2). (a) Asymmetric unit, (b) 1D structure, (c) 2D structure and (d) 3D network formed by the adjacent 1D ribbons in (c) which is marked by the green colour view along the (110) crystallographic direction. (e) shows the C-H \cdots π interactions are shown as orange dashed lines; (f) is the packing framework view along the (110) crystallographic direction.

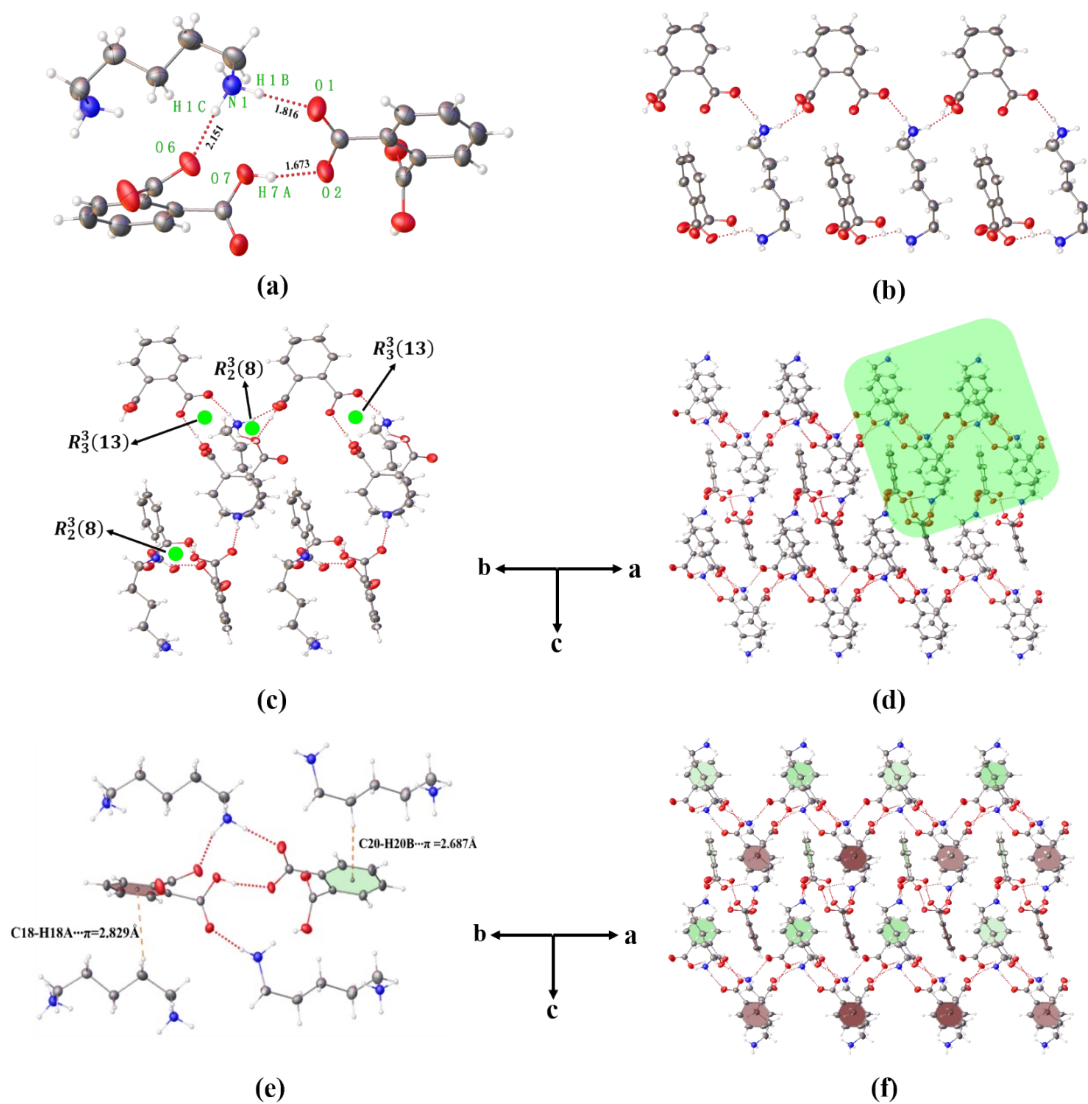


Figure S5 The PXRD patterns of anhydrate-I at different temperatures for long time (A) and different relative humidities for six months (B). (C) The PXRD of five solid forms treated at 120 °C for 3 h, showing that the four crystalline forms can transform to the anhydrate-III except for the anhydrate-I. (D) illustrates that anhydrate-III has extremely stable at different high temperatures.

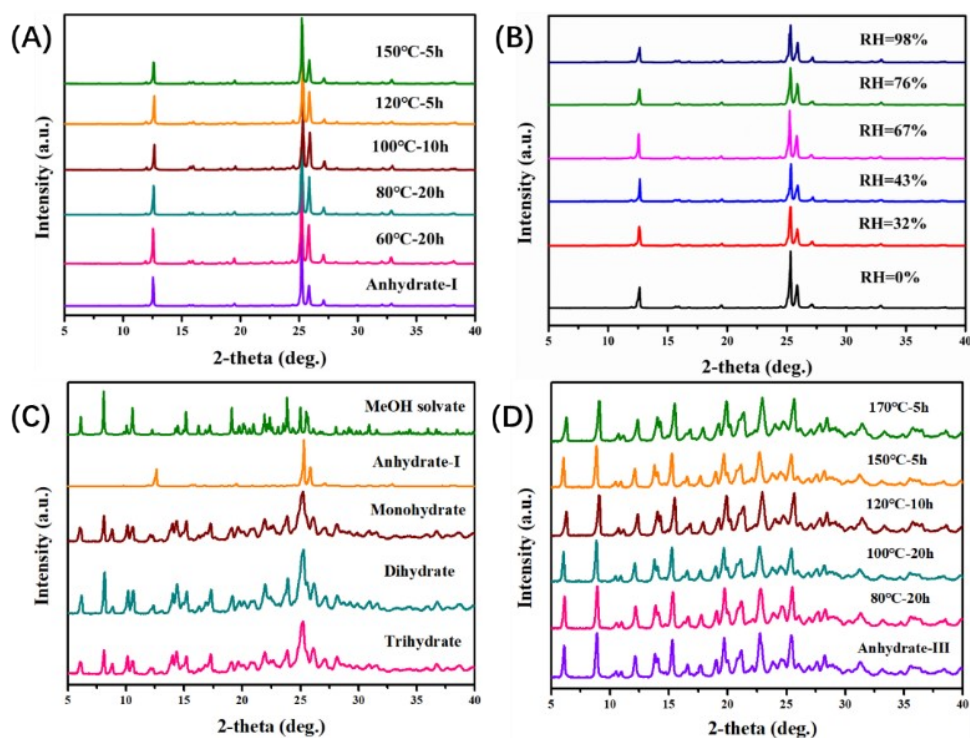


Figure S6 The PXRD patterns of five solid forms at DMF solvent for 12 h, shows that the four pseudopolymorphs of PDA-OPA can convert to the anhydrate-III through solvent transformation.

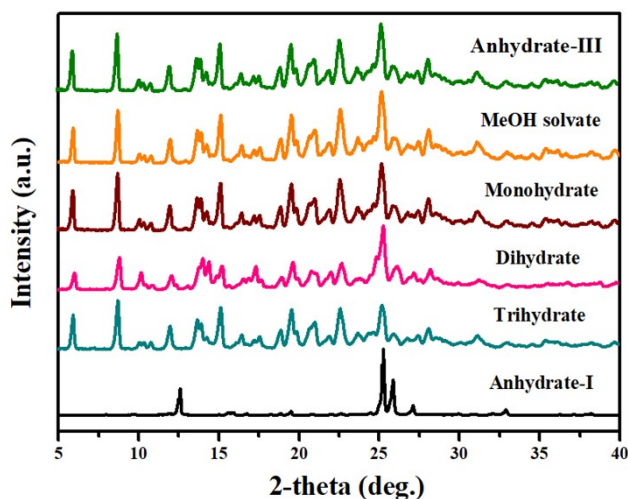
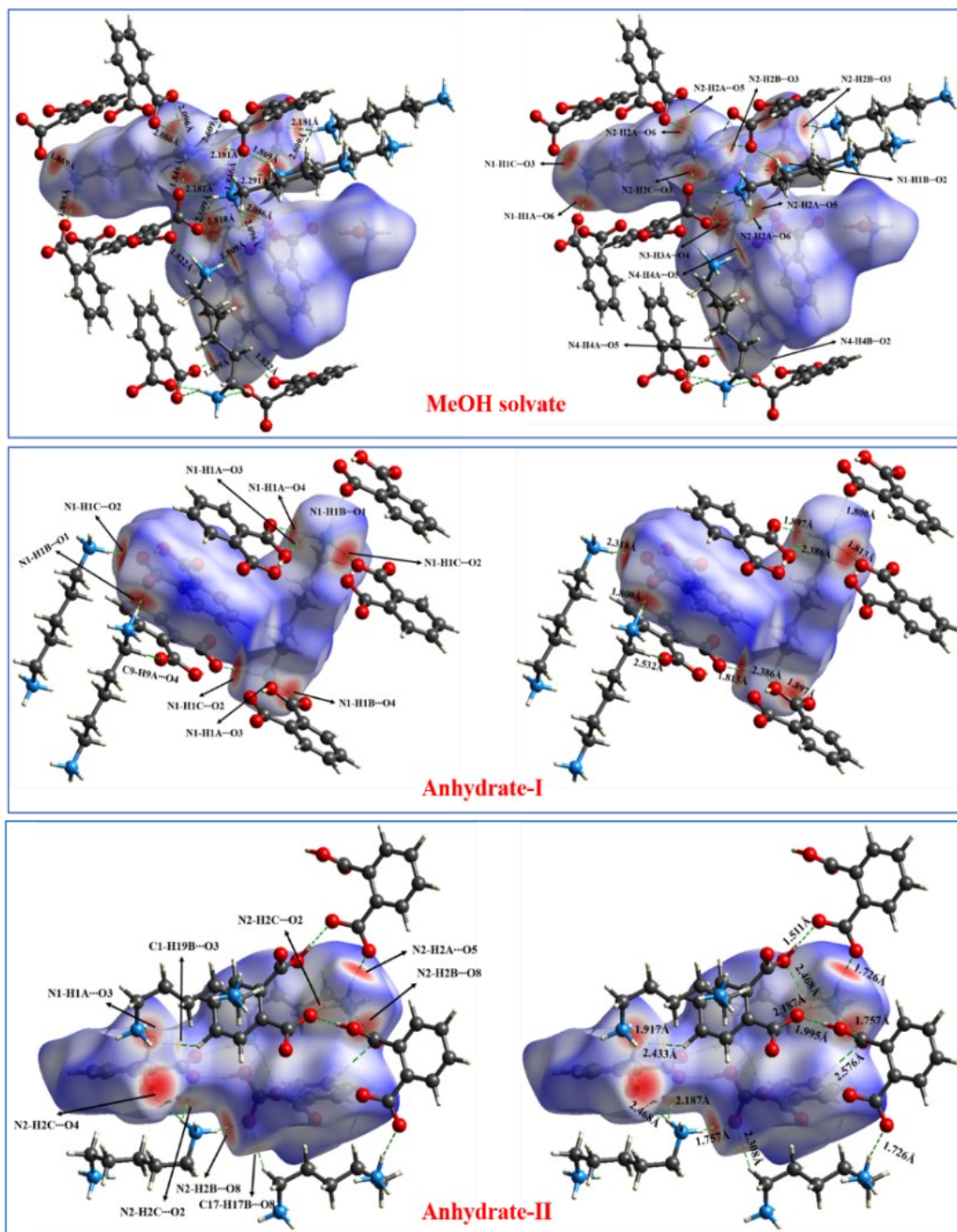


Figure S7 The Hirshfeld surfaces of PDA-OPA mapped showing the hydrogen bond contacts with the $\text{N-H}\cdots\text{O}$, $\text{O-H}\cdots\text{O}$, $\text{C-H}\cdots\text{O}$ in the six solid forms.



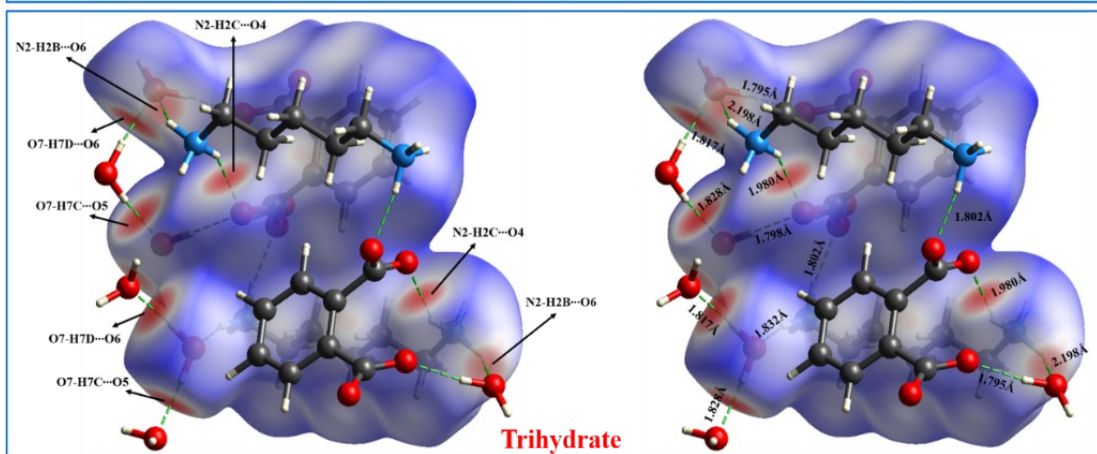
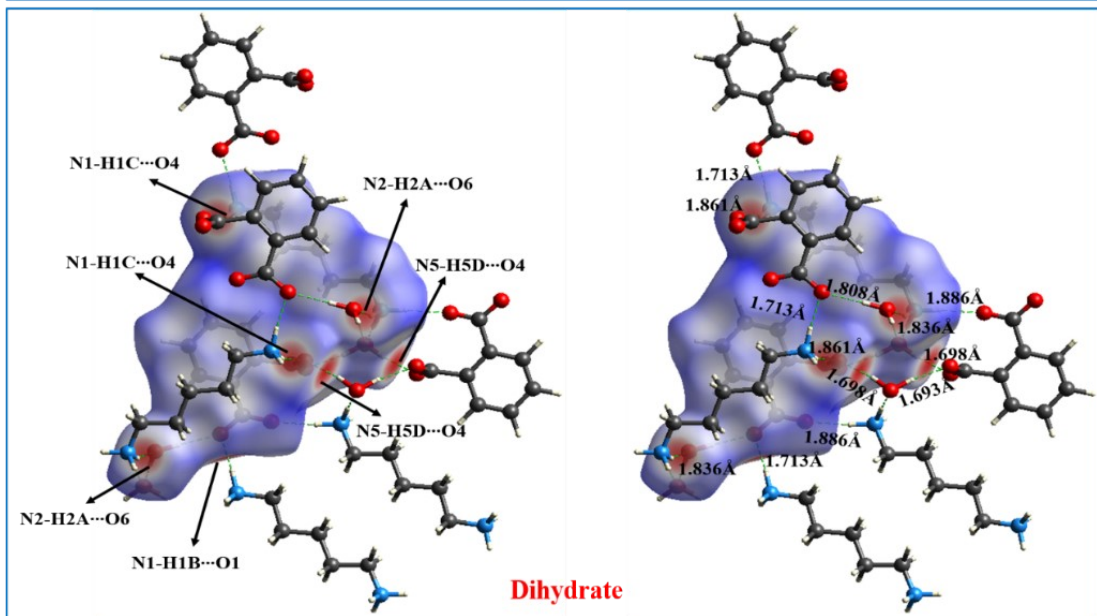
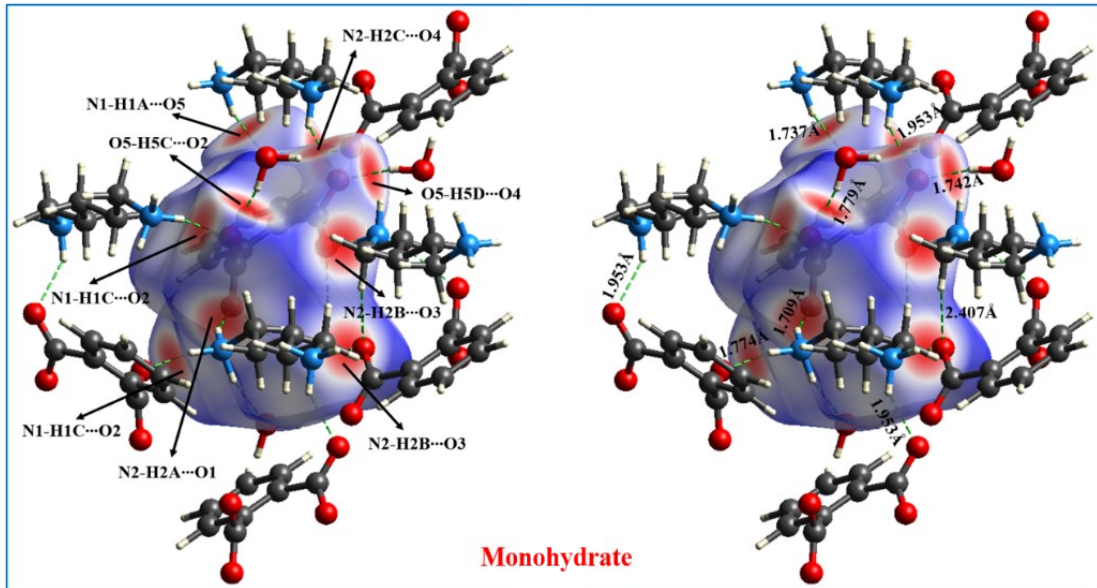
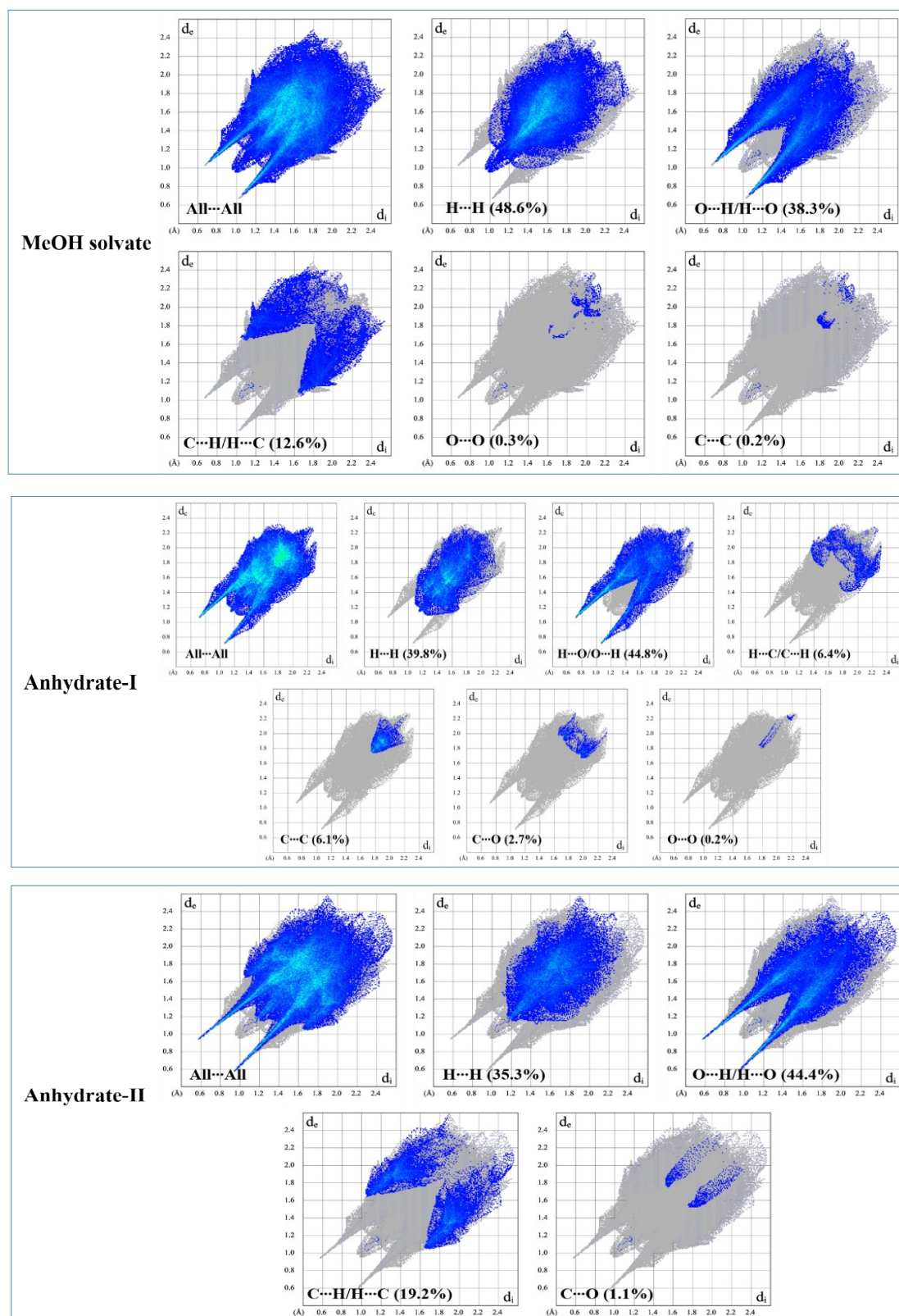


Figure S8 2D fingerprint plots and corresponding contacts contributions of the PDA-OPA pseudopolymorphs and two anhydrous phases.



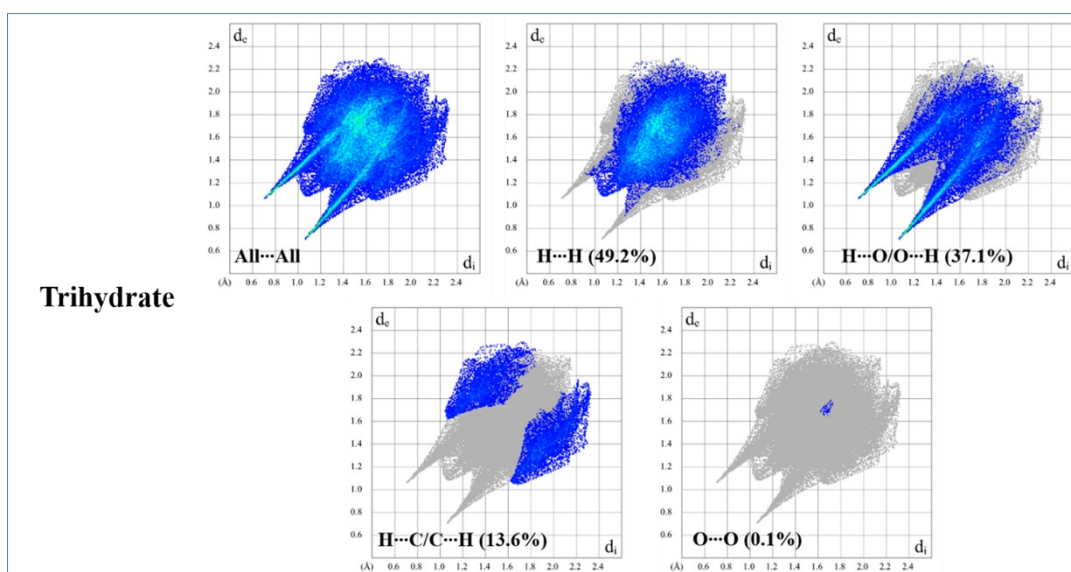
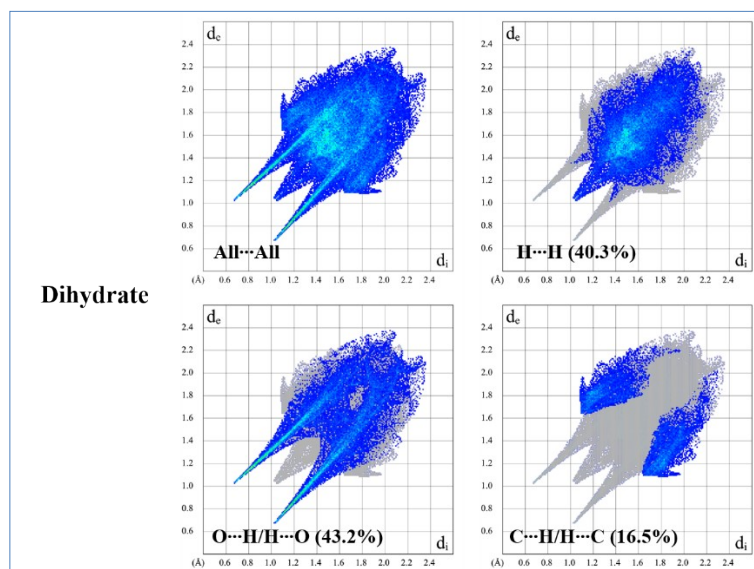
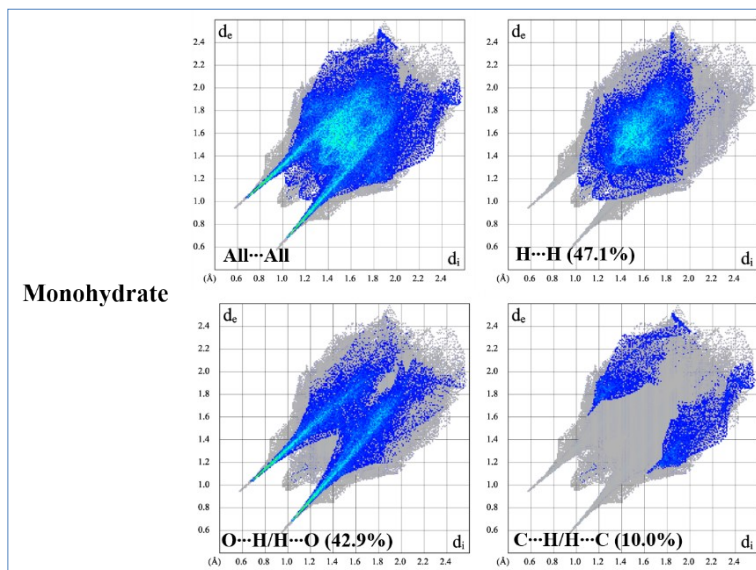


Figure S9 C-H \cdots π contacts in Hirshfeld surface shape index of PDA-OPA pseudopolymorphs: (a) MeOH solvate; (b) anhydrate-II; (c) monohydrate; (d) dihydrate; (e) trihydrate.

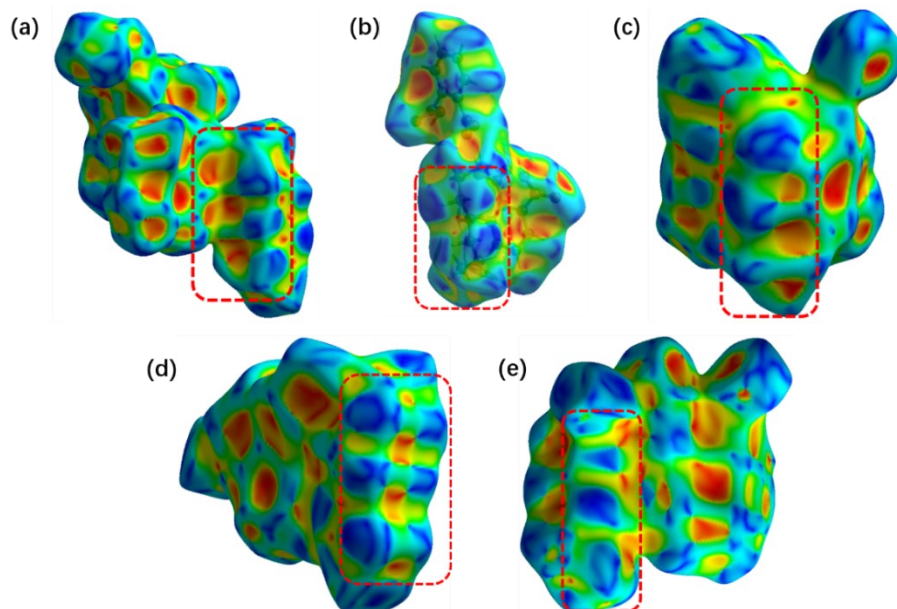


Figure S10 $\pi\cdots\pi$ interactions in Hirshfeld surface shape index of PDA-OPA MeOH solvate (a) and anhydrate-I (b).

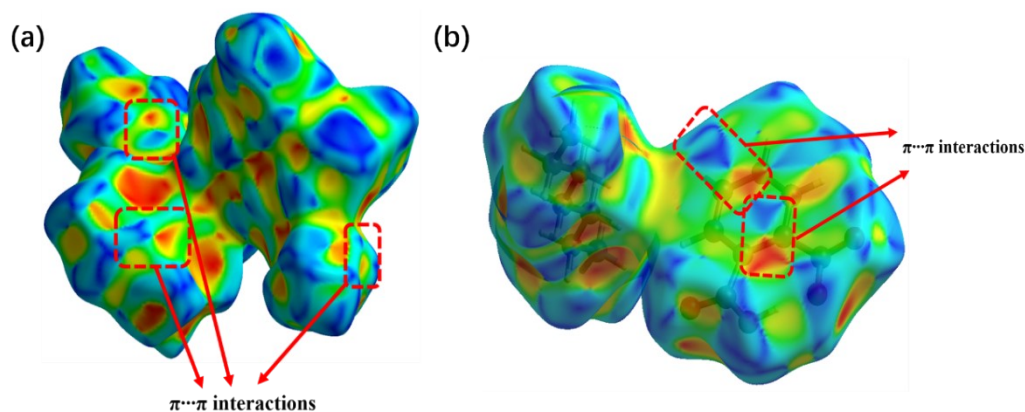


Figure S11 Energy frameworks for the four PDA-OPA pseudopolymorphs and two anhydrous phases, showing the electrostatic (left, red), dispersion (middle, green) and total interaction energy (right, blue). The cylinders corresponding to energies < 2 kJ mol $^{-1}$ were omitted for clarity.

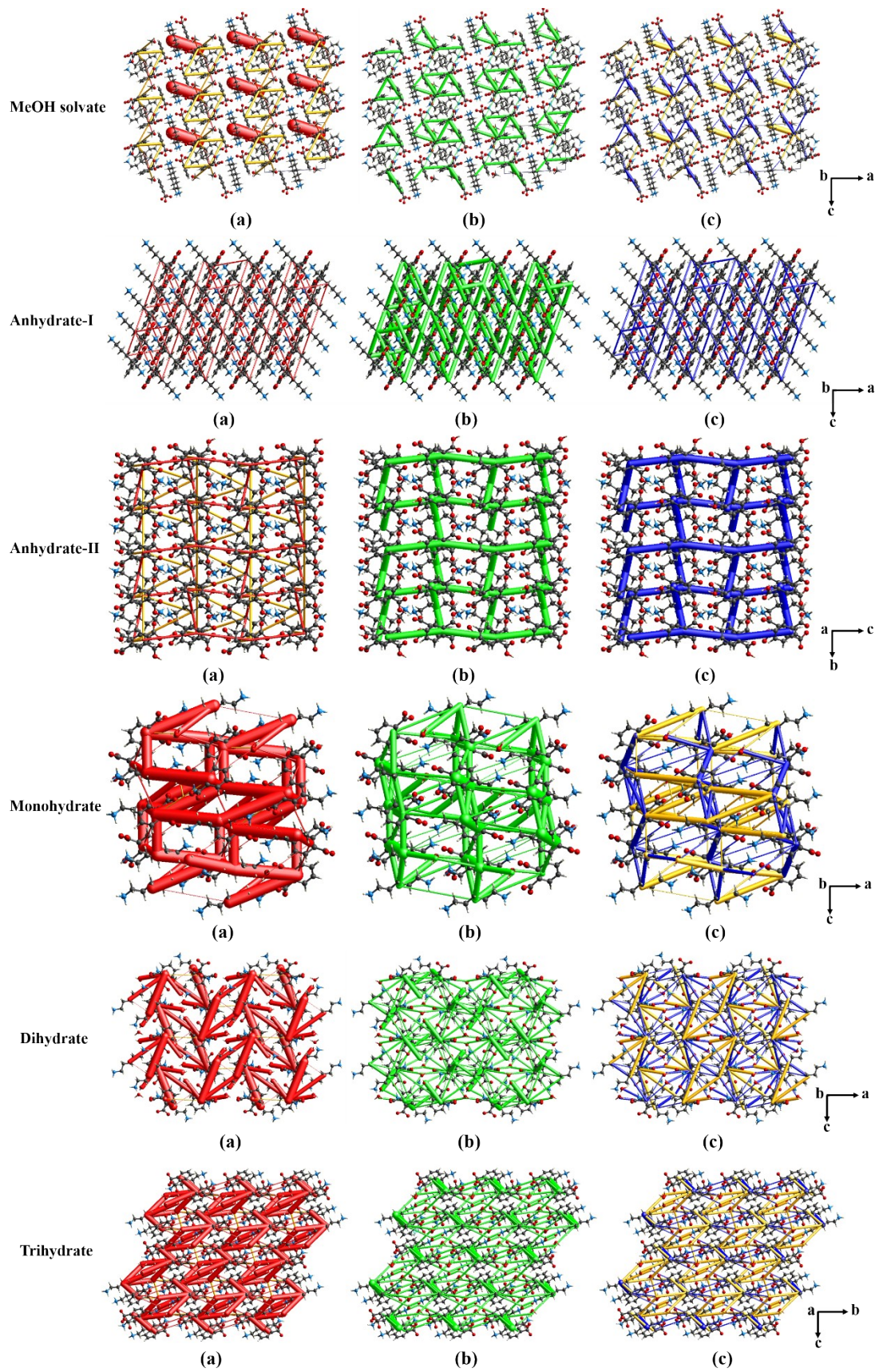


Figure S12 IRI analysis of PDA-OPA two anhydrous phases. (a) is the anhydrate-I and the (b) is the anhydrate-II, (c) is the packing codes of the anhydrate-I. The colored isosurfaces between the two OPA molecules with blue and green, implying attractive interactions arising from a $\pi \cdots \pi$ stacking interaction existing here.

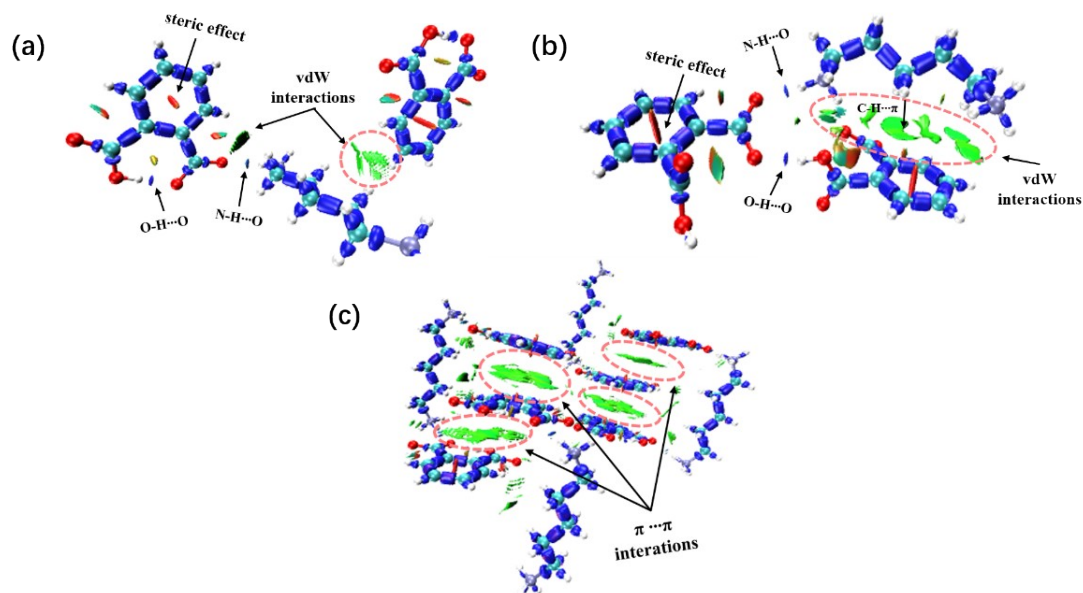


Figure S13 TGA-DSC curves of two anhydrous phases of PDA-OPA salt. (a) is the anhydrate-I and the (b) is the anhydrate-III. The broad endotherm along with a major weight loss, which may be attributed to a combined effect of melting and decomposition.

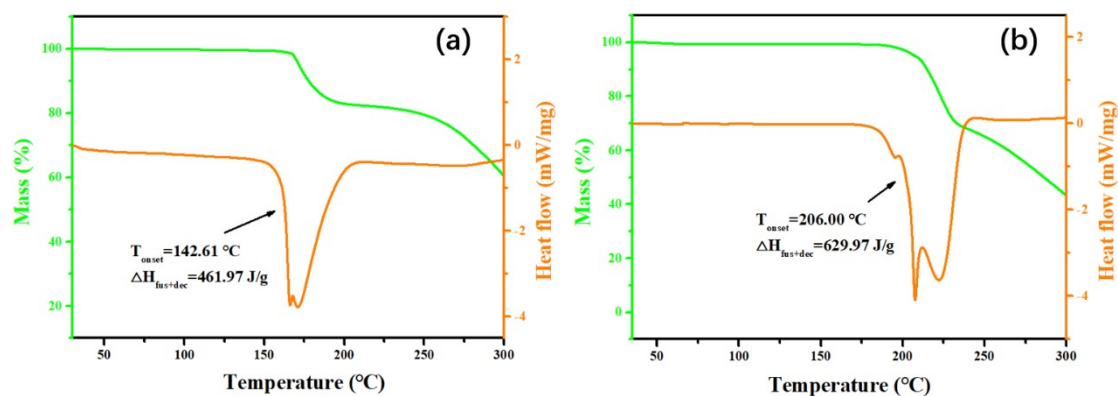


Figure S14 HSM photos of the PDA-OPA pseudopolymorphs. (a-d) are the MeOH solvate, monohydrate, dihydrate and trihydrate, respectively.

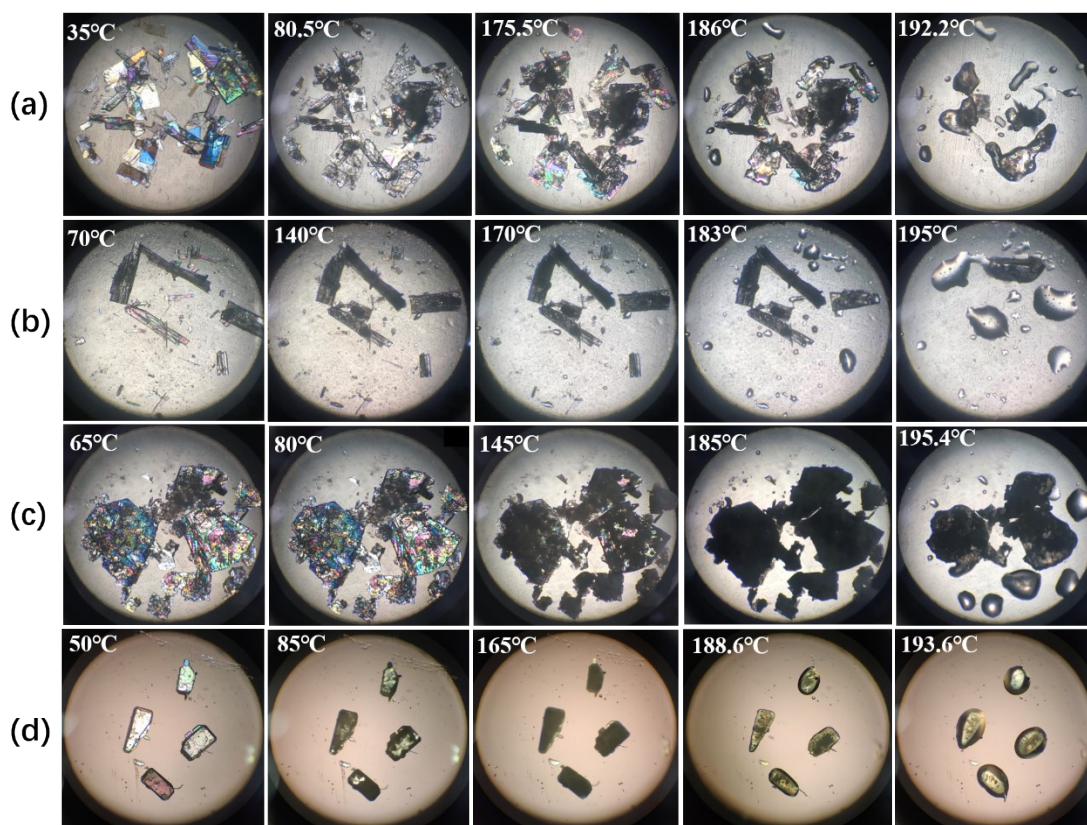


Figure S15 Hygroscopicity of four PDA-OPA pseudopolymorphs under the surrounding conditions with different relative humidity.

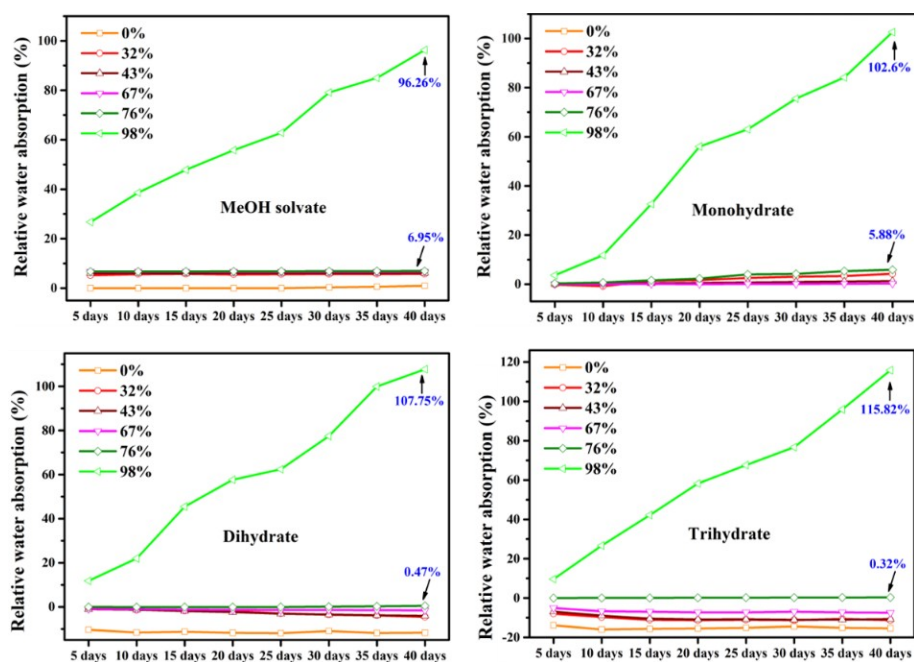


Figure S16 Hygroscopicity of two PDA-OPA anhydrous phases under the surrounding conditions with different relative humidity.

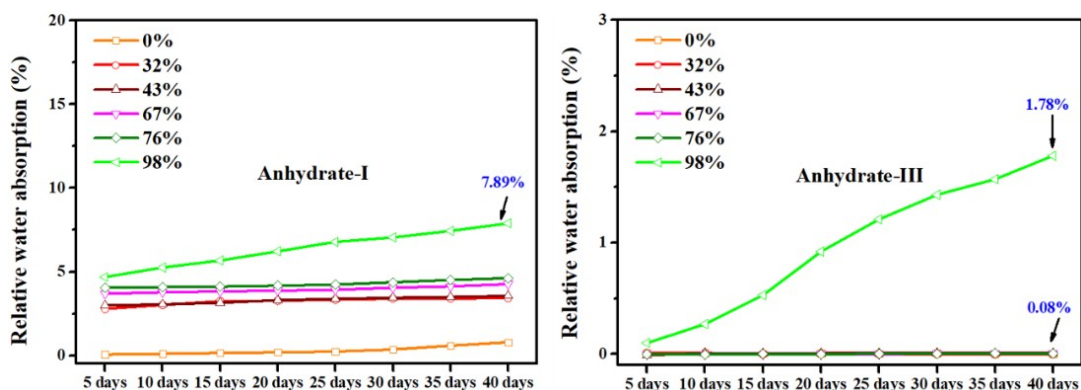


Figure S17 Comparison of the hygroscopicity of six PDA-OPA crystal forms under the relative humidity 98%.

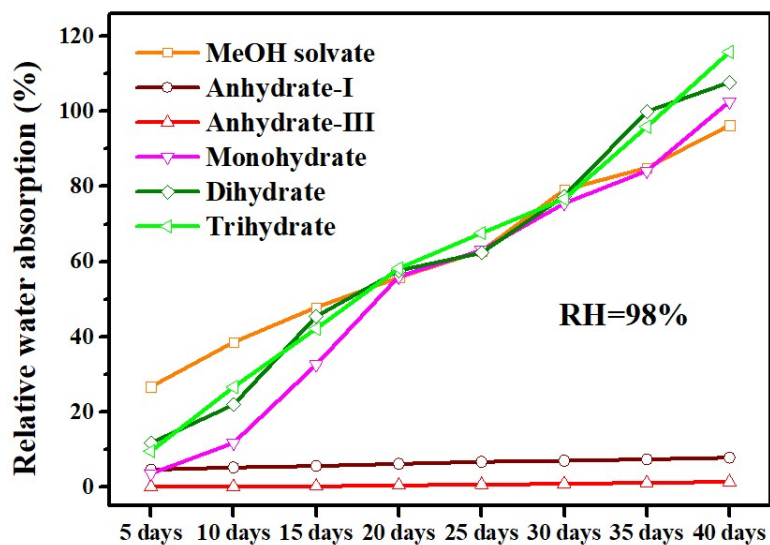


Figure S18 Results of slurry experiments of anhydrate-I and anhydrate-III in different solvents.

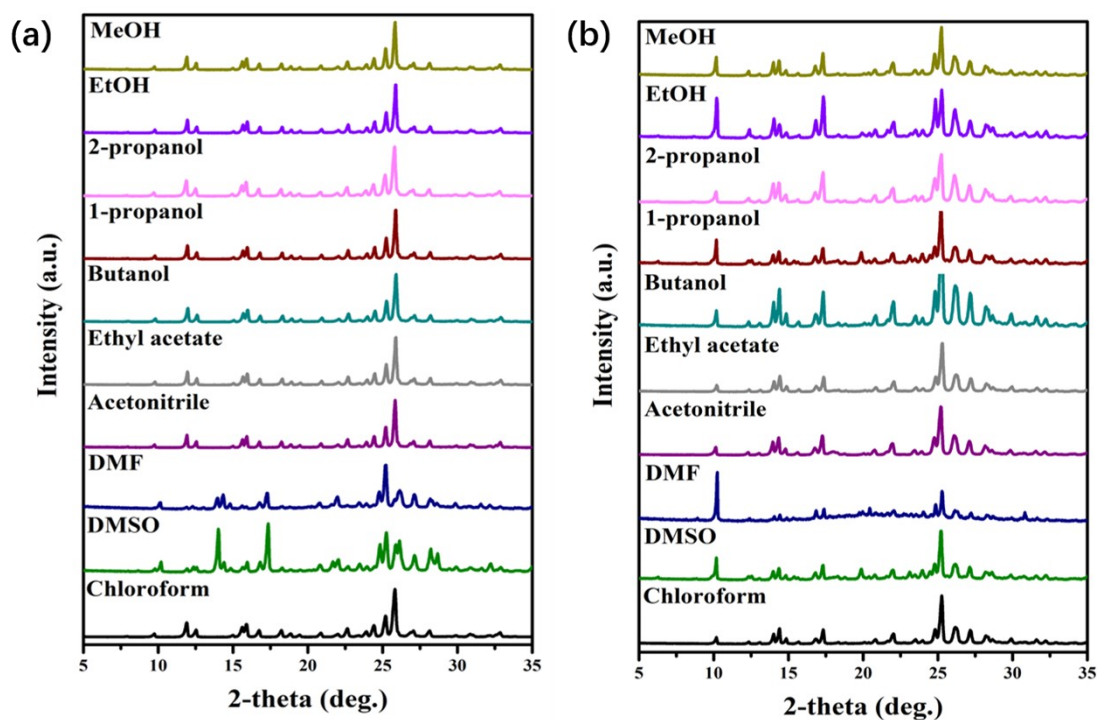
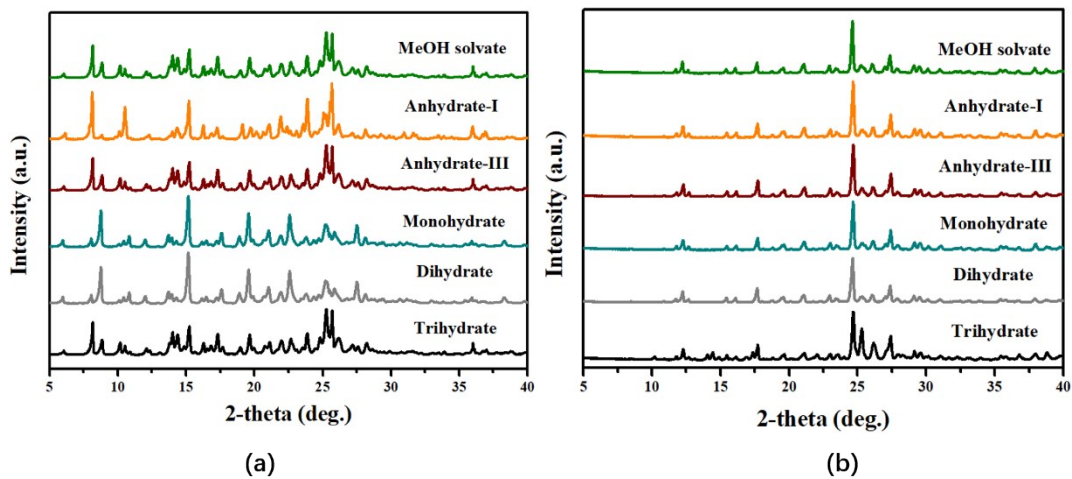


Figure S19 The transformation results of pseudopolymorphs of PDA-OPA in pure methanol (a) and water (b).



The methods for the preparation of three anhydrous forms obtained accidentally:

1. Anhydrate-I: a total 1.8 ± 0.05 g of the PDA and 5.85 g OPA (PDA:OPA=1:2 molar ratio) was completely dissolved in 50 ml and 100 ml of ethanol respectively. Poured PDA-EtOH solution into a 250 ml double-jacketed crystallizer at 70 °C and then, OPA-EtOH solution was slowly added into the crystallizer at a constant rate of 1.0 ml/min by a peristaltic pump. The solution was agitated at 200 r/min and maintained at 70 °C. After all acid solution pumped, the system begins to cool down to 50 °C at a rate of 2 °C/min, then flake anhydrate-I crystals were obtained.

2. Anhydrate-III: weighted 1.8 ± 0.05 g of the PDA and 2.93 g OPA (molar ratio of PDA:OPA=1:1) were completely dissolved in 50 ml and 100 ml of isopropanol, respectively. Subsequent procedures were the same as the former, only difference is that the crystallization process was carried out at room temperature. After filtering and air drying in a vacuum oven at 40 °C for 10 hours, we finally obtained the anhydrous-III powders.

3. Anhydrate-II: However, what we can obtain is only the flake anhydrate-II single crystal through the slow solvent evaporation from the supersaturated solution of anhydrate-III. Thus, it can only be analysed through its crystal structure of anhydrate-II, but its physicochemical properties cannot be characterized.